Design and Optimization Strategy to Size Resilient Stand-Alone Hybrid Microgrids in Various Climatic Conditions

Article · August 2022

DOI: 10.1109/OJIA.2022.3201161

4 authors, including:

Norma Anglani
University of Pavia
63 PUBLICATIONS **756** CITATIONS

SEE PROFILE

Giovanna Oriti
Naval Postgraduate School
63 PUBLICATIONS **1,316** CITATIONS

SEE PROFILE

Douglas Lee Van Bossuyt
Naval Postgraduate School
106 PUBLICATIONS **441** CITATIONS

SEE PROFILE

Design and Optimization Strategy to Size Resilient Stand-Alone Hybrid Microgrids in Various Climatic Conditions

Norma Anglani, *IEEE Senior Member*, Giovanna Oriti, *IEEE Senior Member*, Ruth Fish, and Douglas L. Van Bossuyt

***Abstract*—This paper presents an original two-steps methodology to size DERs (Distributed Energy Resources) in stand-alone microgrids, to be installed in different areas, featuring different meteorological conditions, but same kind of loads. Design examples are simulated to analyze how an increased level of resilience, considered in terms of number of days of autonomy after an initial incident, affects the sizing of a PV field and its storage. A practical tool to support strategic choices is methodologically illustrated and applied to two case studies to find the best configuration, which is identified by a trade-off among fuel consumption, sizes of PV arrays and resilience. Key design parameters help in designing the best system according to the location, by focusing on the newly identified key performance indicator NPV^s, the simplified net present value of specific scenarios of interest, where a penalty is introduced to account for less than the ideal target of autonomy. The model-based design used to create the microgrid simulations is validated by experimental measurements on a test-bed hybrid microgrid.**

***Index Terms*—stand-alone microgrid design, resilience, DER integration, EMS, PV, batteries, decision support strategy, climatic conditions, design optimization.**

NOMENCLATURE

α, r: fraction of critical over daily load, discount rate (p.u.)
c_f, AFC: fuel cost (\$/gal), annual consumption (gal/y)
C_r, C_r^L, C_r^{CL} storage capacity for: total, daily and critical load (kWh)
c_{PV}, N_{PV}: PV cost ($\$/kW_P$); # PV panels
c_P, c_{bat}: penalty and ESS specific cost (\$/kWh)
F_{bat} costs for storage (\$)
NPV^s net present value (simplified)
P_{PV}, P_L, P_{CL}: peak power (kW_P), daily load, critical load (kWh/day)
T_H time horizon (years)
ALR array to load ratio (p.u.)
$CAPEX, OPEX$: capital (\$), annual operating expenditure ($\$/y$)
DG diesel generator
DoA Days of Autonomy (days)
PSH peak sun hours (kWh/(m^2.day))
SF solar fraction (p.u.)
SoC state of charge (p.u.)

Funding partially provided by NAVFAC Naval Shore Energy Technology Transition and Integration (NSETTI) program.

Manuscript received Month xx, 2xxx; revised Month xx, xxxx; accepted Month x, xxxx. This work was supported in part by the xxx Department of xxx under Grant (sponsor and financial support acknowledgment goes here).

(Authors' names and affiliation) First A. Author1 and Second B. Author2 are with the xxx Department, University of xxx, City, Zip code, Country, on leave from the National Institute for xxx, City, Zip code, Country (e-mail: author@domain.com).

Third C. Author3 is with the National Institute of xxx, City, Zip code, Country (corresponding author to provide phone: xxx-xxx-xxxx; fax: xxx-xxx-xxxx; e-mail: author@ domain.gov).

I. INTRODUCTION

Military operations across the globe require mobile camps with stand-alone power systems, which cannot rely on local utility grids. Recent advances in photovoltaic (PV) sources and energy storage systems (ESS) have resulted in the use of these distributed energy resources (DERs) [1], which require careful sizing in different geographical locations. The goal of this paper is to provide a novel decision support strategy (DSS) which compares the key design parameters, used in the sizing of a hybrid microgrid, with respect to environmental factors, fuel consumption, resilience, and economics.

Resilience, in the context of microgrids supporting military missions, is generally defined as the ability to supply critical loads over a specific number of days (generally 14 days) during a disturbance such as several cloudy days blocking PV electricity production, adversary action that destroys a microgrid component, or the inability of diesel fuel to be resupplied [2]. The number of days of microgrid operation is tied to how long it takes an unaffected military facility to take over national security functions of the affected facility. An important consideration when developing a resilient military microgrid is the potential for multiple disturbances to happen over a 14 day period such as multiple hurricanes impacting a base. Thus it is important for a military microgrid to quickly recover after an initial disturbance in order to be ready for another disturbance.

The use of powerful and complex optimization techniques is very popular in energy planning and controls; however, no overall methodology which focuses on resilience from the simulation of a stand-alone microgrid down to the most cost-effective results is currently available in the literature, as far

as the authors are aware. This paper presents a methodology which requires a somewhat limited computational time and is implemented in two steps: 1) design and simulations, 2) selection strategy according to the identification of an indicator and 3) trade-off analysis.

A. Literature review

The use of optimization methods to size the DERs in microgrids has been well documented in recent papers such as [3]–[6]. In [3] off-grid microgrids with various combinations of PV, battery and diesel are sized using a "two-stage particle swarm optimization algorithm", with the goal to minimize the power system's overall cost. Optimal DER sizing with multiple objectives was also presented in [4] for grid-connected residential microgrids and in [5] for zero-energy buildings, factoring various climatic and environmental parameters. Although geographical location and environmental impact were considered in [4] and [5] respectively, the microgrid's connection to the main grid, and the utility's tariffs play a major role in their optimization algorithms. Reliability, which contributes to resilience, is the focus of the offline mixed integer linear programming (MILP) optimization method presented in [6]. A comparison of optimization algorithms is presented in [7], where the authors conclude that the "hybrid Whale Optimization Algorithm" yields the best results.

While these papers propose several methods and algorithms to optimize for cost when introducing renewable energy sources and storage into a microgrid, none of the proposed design methods allows for a design to maximize resilience in locations with different climatic conditions.

Reliability and resilience have been very recently addressed in microgrid literature [8]–[11] with complex, iterative sizing and energy management methodologies, requiring much time and operator knowledge to yield the promised results. For instance in [12] a MILP (mixed integer linear programming) problem is implemented to maximize delivery of power to critical loads after an extreme event. In [13], resilience is analyzed by using a multiobjective approach, which aims at optimizing the solar allocation and the batteries as well as minimizing costs and access to the supply side. Three main objectives are balanced: the investment and operation costs; the capacity accessibility for electricity demand; and for the generating units. This paper is interesting in the approach although it offers a different formulation for resilience. In general the majority of the literature focusing on resilience of a grid, look at microgrids as possible backups for the main, as also observed in [14]. A recent paper [15] provides a similar approach to ours, but the aim is to demonstrate that an hybrid microgrid configuration (diesel generators -DGs- supported by DER and ESS) is by itself more resilient than that only supplied by DGs.

B. Specific contribution

The scope of our work, instead, is to investigate further by considering how to assess the role that increased storage can play and how to trade-off among the many conflicting issues [16], expanding on what in [15] the authors show as a resilience concept, though differently defined: the hybrid microgrid.

For this reason it is worth offering an overview of what resilience can mean. Five distinct time periods can be identified: 1) pre-disturbance where the system is operating nominally, 2) disruption where the system has suffered a disruptive event as is actively degrading to a degraded state that is below acceptable operating thresholds, 3) full impact where the system experiences the full impact of the disruption for some period if time, 4) recovery where the system is recovering to an acceptable operating threshold (full recovery to often pre-disturbance operations but sometimes a partial recovery lower operating state that is acceptable to stakeholders), and 5) post-recovery [17]. Many variations on how resilience is decomposed exist including more complex and finely defined time periods and states, and less complex [18], [19]. For the purposes of this research, we focus on the period of time the load is without power from DGs and PV (the full impact of the disruption) and the period of time after power is restored that it takes for the ESS to recharge fully to be prepared for the next disruption (the recovery). These two periods of time are most important to military microgrids because military planners must understand how long an outage may last and how long it may take to be prepared for the next disruptive event [2]. The paper is organized as follows: in section II the design methodology and examples for different climatic conditions are presented. In Section III the chosen strategy to achieve the desired level of resilience is explained and the steps to achieve the results of the trade-off methodology are detailed. Section IV presents the experimental validation of the model and the final remarks are included in Section V.

II. First Step: DER Sizing and Selected Design Examples

A microgrid sizing methodology was developed, expanding on the design tool presented in [20] by adding DGs to the microgrid architecture and temperature as a design input [21], to better take into account location specific installations. The method includes design equations to size energy resources and a physics-based model to simulate the functionality of the stand-alone microgrid under various environmental and climatic conditions. The design examples presented here are supported by several simulations obtained with a physics-based model reported in [21] and experimentally validated in section IV. DERs are sized for microgrids located in Fairbanks, Alaska; San Diego, California; and Rota, Spain, although for a matter of space we will focus the results only on the first two cases. The system and load specifications, battery model, days of autonomy (DoA) for the critical load, PV model, array to load ratio (ALR) [20], use of maximum power point tracker (MPPT), and DG design were the same for each microgrid in the 3 locations. As a result, PV sources are sized differently in each location as shown in Figure 1, where the number of PV arrays is displayed versus the solar fraction (SF) for 30 microgrids designed with 4 DoA in the month of February, later referred as PSH2-sizing. SF is a number

between 0 and 1 which determines how much of the average daily load energy will be provided by the PV arrays based on solar energy available during the selected design-month. DoA is the number of days the battery is designed to support the identified critical load if all other DERs (here DGs and PV) are unavailable. The simulations covered one year in each location and, if we emphasize on the role that location can play, the expected dramatically larger number of PV panels can be observed in Fairbanks, due to the reduced solar irradiance at that latitude.

The outputs of the first design example are shown in Figure 2, where the annual fuel consumption (AFC) is plotted for each location for 10 different SF designs, according to a sample Peak Sun Hours (PSH) (for instance, for Fairbanks is 0.8 kWh/(m^2.d), associated to February). Over the course of one year, in each location the AFC in gallons remains relatively constant as the SF decreases from 1 down to 0.5 SF, when it spikes up.

In fact, the increase in fuel usage of the 0.6 SF system from the 0.9 SF system in Fairbanks is just 96 gallons or 7.3% of the 0.9 SF system fuel usage which is equal to ≈ 1200; while the different in size between the 0.6 SF and the 0.9 SF systems is 855 PVs, or a 25% decrease. The increase of fuel usage of the 0.4 SF system from the 0.6 SF system is 298 gallons or 21.2% of the 0.6 system fuel usage; while the difference in size between the 0.4 SF and 0.6 SF system is 846 PVs, or a 33% decrease. This suggests that the percentage of fuel saved by increasing the number of PVs decreases as the size gets closer to that of the 1.0 SF system: still the best trade-off needs to be found.

We recall that similar SF means that we can equally provide the same amount of load but this happens with a different PV numbers in each location. So, the location mainly affects the size of the PV field, which in turns affects the consumption. Less critical issues seem to have the sizing in the other two locations.

A second design example focuses on resilience by simulating the rate of recovery, defined as the rate which the battery charges while supporting the load, without a DG on a sunny day. The simulated results are shown in Figure 3 where the battery annual charge rate in $\%$ is plotted as a function of the SF for the three locations.

This design example assumes the DG unavailable and the batteries partially depleted at the begin of the simulations, with SOC of 30% which are appropriate assumptions when examining the microgrid's resilience to a second disturbance. While a smaller SF means a lower initial cost, the average rate of recovery is negative below a certain SF. With a small enough SF, the system cannot support the load without DG throughout the entire year. Note that in California and Spain, where the solar irradiance has less variations over the year, the charge linearly increases with SF, thus resulting in reduced resilience of the designs with lower SF compared to the microgrid designed for Fairbanks. In other words, the less variation there is in solar irradiance throughout the year, the higher the SF of the hybrid PV microgrid must be to operate on solar power and battery storage alone (ESS) for the majority of the year.

Conversely, the greater variation there is in solar irradiance throughout the year, the more reasonable it is to use a lower SF, while still supporting the load with primarily solar power and conserving initial cost. The simulation results presented here show some trends but they do not identify an optimal DER sizing. The second step of this methodology will help identify the best configuration or the best trade-off among lower fuel consumption and increasing number of PV panels. From these preliminary results it is not yet clear how a different design-month affects the microgrid's resilience, because costs are not introduced yet. Finally, the role of storage and how it affects the DoA is not linked to any useful criteria for driving the choice. A flowchart of the process used in this first step is shown In Fig. 4.

III. Second Step: Decision Support Strategy (DSS) and Trade-Off Analysis

The DSS presented in this section determines how to best size the microgrid according to the various effects stemming out from each sizing strategy. Investments and operating costs are key-points, but the novelty relies on the significant key performance indicator (KPI), driving the most suitable choice. The design examples presented above depend on the SF and DoA as well as on the month taken as a reference for the design of the PV source. The design month determines the PSH and temperature [20], and it impacts the AFC (Annual Fuel Consumption), as well as the operating of the ESS, although it is not a key point in the current analysis. Additionally, the higher the DoA the more resilient the microgrid to both initial and secondary disturbances, the bigger the battery, and the higher the initial cost. In this section we consider all the goals an energy manager has to account for in the microgrid design and subsequent management, i.e. minimizing AFC, maximizing DoA, maximizing the PV production while keeping ESS size and cost as low as possible, and propose a practical DSS.

Although military microgrid design prioritizes energy security (and the sizing of the battery strictly must follow this principle), cost is also an important parameter to consider. Thus, we propose to start from the NPV (Net Present Value) of the CAPEX (CAPital EXpenditures), the OPEX (OPerating EXpenditures), annualized according to a meaningful time frame T_H, and a penalty for the offset between any days of autonomy (DoA) smaller than 14 and add an additional step in the KPI identification. This time frame represents when a potential disruptive event is likely to happen or it can be assumed as an established reference time T_H (in years) to be identified by the facility's energy manager.

Let's consider as CAPEX only those costs associated with what can change in the microgrid configuration: as those due to the capacity of the battery (F_{bat1}) and extension of the PV field (F_{PV}). The latter depends on $c_{PV} * N_{PV} * P_{PV}$, with c_{PV} a specific cost over peak power, N_{PV} and P_{PV} the number and power rating of PV arrays respectively. For the battery the overall cost (F_{bat}) is made up not only of the CAPEX, proportional to the rated capacity C_r, which in turn depends on the DoA ($F_{bat1} = c_{bat} * C_r(DoA)$), but also of F_{bat2} a term related with a penalty (c_P, in \$/kWh).

This article has been accepted for publication in IEEE Open Journal of Industry Applications. This is the author's version which has not been fully edited and content may change prior to final publication. Citation information: DOI 10.1109/OJIA.2022.3201161

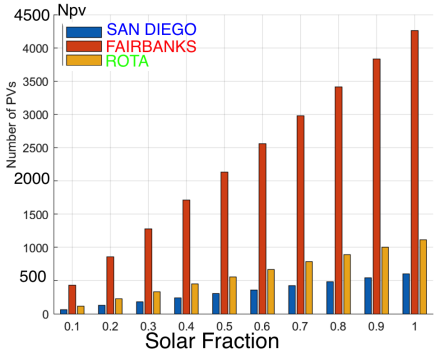

Fig. 1. N_{PV} (# of PV panels) vs SF, for a sample PSH

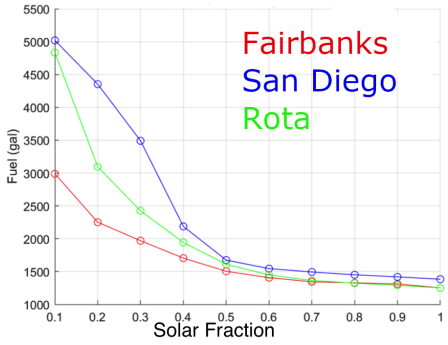

Fig. 2. Consumption: AFC (gal/y) vs SF

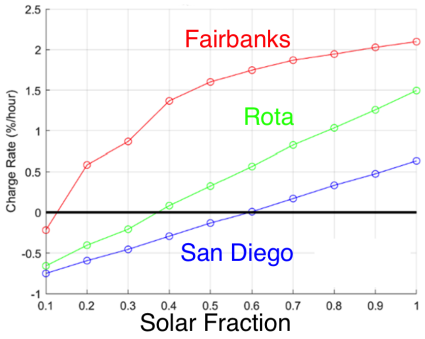

Fig. 3. Average annual charge rate vs SF

Actually, $C_r(DoA)$ is the overall capacity needed to assist the PV daily production in NOC, normal operating conditions (C_r^L) and, for the most part, to support the critical load, in case of a disruptive long-lasting event (C_r^{CL}), thus:

$$C_r(DoA) = C_r^{CL}(DoA) + C_r^L \tag{1}$$

Here, the resilience, represented by the autonomy on 14 days appears in the battery sizing.

The penalty F_{bat2} represents the cost of taking the risk to size the system for less than the targeted 14 DoA on the critical load. So we will have:

$$F_{bat} = F_{bat1} + F_{bat2} \tag{2}$$

$$\begin{aligned} F_{bat} = [c_{bat} * C_r(DoA)] + [c_P * \Big(C_r^{CL}(DoA_{=14}) + \\ -C_r^{CL}(DoA)\Big)] = \\ +c_P * C_r^{CL}(DoA_{=14}) + c_{bat} * C_r^L + \\ cbat * C_r^{CL}(DoA) * \left(1 - \frac{c_P}{c_{bat}}\right) \end{aligned} \tag{3}$$

$c_P * C_r^{CL}(DoA_{=14})$ -as well as the DGs' capital cost- have the same value in each investigated scenario, thus we can neglect it from the NPV assessment of Eq.4, thus introducing F_{bat}^s (simplified F_{bat}), which is an intermediate step towards the definition of our ultimate KPI. Conversely the cost of the diesel consumption is considered as the only annualized OPEX ($c_f * ACF$, with r discount rate over time T_H), remembering that the higher the discount rate, the lower the value we assign to future savings in today's decisions. Once the load (P_L) (as well as the strategy on the critical loads where P_{CL}=α*P_L and $\alpha \leq 1$), the ALR, the unitary investment costs (c_{bat}, c_{PV}) are all set, in each location j, then:

$$\begin{aligned} NPV\Big(F(SF, PSH, DoA, c_P, c_f)\Big)^s = \\ F_{PV} + F_{ACF} + F_{bat}^s \end{aligned} \tag{4}$$

$$\begin{aligned} NPV(F(SF, PSH, DoA, c_P, c_f))^s \\ = [c_{PV} * N_{PV}(SF, PSH) * P_{PV}] \\ +[c_f * ACF(SF, PSH) * \frac{1}{(1+r)^i}] \\ +[c_{bat} * C_r^L + c_{bat} * C_r^{CL}(DoA)(1 - \frac{c_P}{c_{bat}})] \end{aligned} \tag{5}$$

the last term, in the third square bracket of Eq. (5), tells us that, to the fullest extent, to keep NPV low, when c_P is bigger than c_{bat}, then $C_r^{CL}(DoA)$ has to raise to its maximum, which is $C_r^{CL}(DoA_{=14})$ -the capacity for the full autonomy of the critical load on 14 days. Nonetheless, if c_P is lower than c_{bat} (the most meaningful cases to investigate), then $C_r^{CL}(DoA)$ could strive to lower values. The capacity C_r^L depends only on how the daily PV production is assisted by the storage in NOC, hence it does not depend on DoA.

Nevertheless, the choice on PV can drive different sizing strategies on C_r^L and both affect the diesel consumption, as well as the recharge strategy, that we neglect here. With respect to α, if α = 1, then the load is all critical, if α =0 then there is no penalty on resilience because critical load is null.

The parameter c_P is to be determined by the energy manager who can appraise how much the undelivered kWh (due to the disruption) can cost to the facility. When c_P is greater than c_{bat} there is no advantage in downsizing DoA below 14 days, if NPV^s is the key decision parameter.

Once we know c_{PV} and c_{bat}, then we can assess all the $SF * DoA * c_P * c_f * PSH$ combinations of NPV^s, so the minimum value:

$$NPV^* = min(NPV(F)^s) \tag{6}$$

will identify which SF, PSH, and DoA (SF^*, PSH^*, and DoA^*) -for any identified meaningful cost c_P-c_f among the many investigated- provide the least cost F^s. Additionally, every chosen PSH affects the role of curtailment of the PV production. The parameter PSH is linked to the design month, which can be chosen as either the month with the worst daily irradiation [22], or other meaningful months as the one considered in Section II.

In Fig. 5, the whole DSS procedure is reported.

A. Results

For the current simulations we chose for Fairbanks the PSH1 and PSH2 of January and September respectively, while for San Diego we selected January and March, respectively. Among many possible choices those were the most significant because, for both locations, January is the second worst solar month (PSH1), thus a large number of PV panels is expected

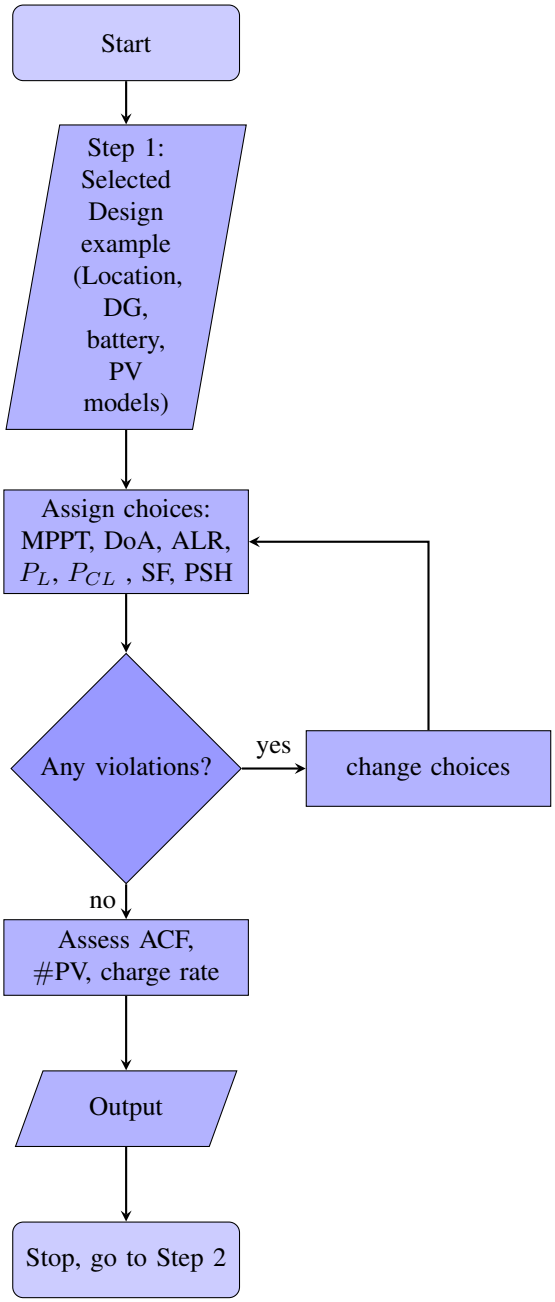

Fig. 4. Flowchart describing Step 1

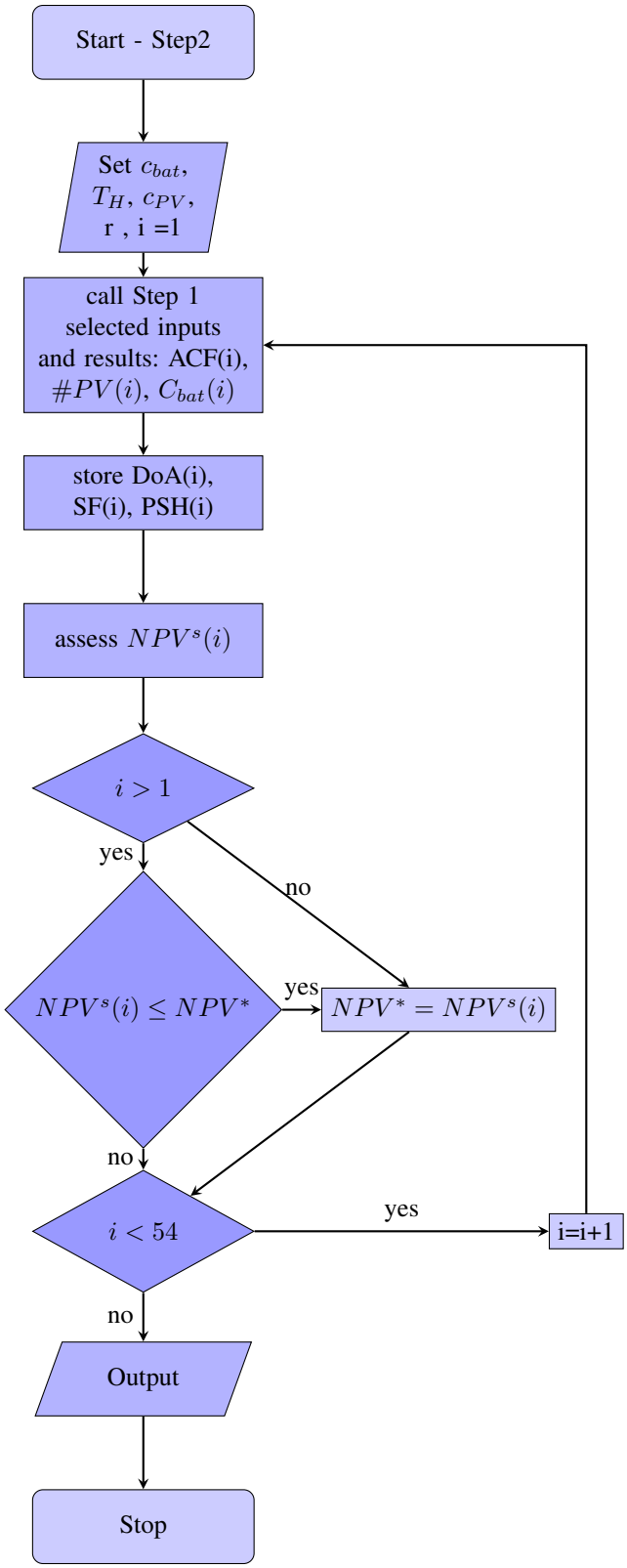

Fig. 5. Flowchart describing Step 2

as well as a relevant curtailment, and PSH2 is the one most similar to the average solar month, then the opposite behavior is expected (less curtailment and fewer PV panels).

The best configuration for location j can be chosen by looking at the minimum value among all the different NPV(F^s) and since NPV^s (the gross number) can be difficult to contextualize by itself, the ratio between $NPV(F)^s$ and NPV^* is also computed (*NPV rate*) to indicate the percentage of savings brought in by NPV^* against the other SF-DoA-PSH solutions: *NPV rate* is thus our ultimate KPI.

This ratio is the chosen key parameter to aid the decision in the following trade-off study which focuses on the two most diverse locations, San Diego and Fairbanks. The study

includes a wide-range, though selected, solutions, which an energy manager should compare when designing a microgrid.

The design input parameters for San Diego, identified as *location1*, and for Fairbanks, identified as *location2*, are summarized in Tab. I, including battery and PV costs (c_{bat}, c_{PV}), battery efficiency (η_{bat}, daily energy consumption of the load (P_L), T_H (time frame) and discount rate r for energy investments. In this example, the critical load is equal to the whole load P_L, thus α is equal to 1.

TABLE I
INPUT DATA AND CHANGING PARAMETERS (IN BOLD) FOR SCENARIO DEFINITION

Set data	definition	units of meas.	range;step
0.1-0.3-0.7	c_p over c_{bat}	p.u.	0.1-1; 0.1
4-10-20	c_f	\$/gal	4-10-20
4-7-14	DoA	days	1-14;1
.14 - 3.	PSH1 (Loc.2, Loc.1)	kWh/m^2.d	
2. - 5.	PSH2 (Loc.2, Loc.1)	kWh/m^2.d	
San Diego	Location1		
Fairbanks	Location2		
360	P_{PV}	W_p	250-360
0.75	η_{bat}	p.u.	0.7-0.99
400	c_{bat}	\$/kWh (Li-ion)	400-600-1000
1200	c_{PV}	$\$/kW_P$	1200-1700
600	$P_L = P_{CL}$	kWh/d	
0.75	η_{bat}	p.u.	0.7-0.99
5	T_H	years	5-20;1
5%	discount rate		4.5-5.5%; 0.5

Hence, a selected number of MonteCarlo simulations have been run by varying the parameters highlighted in Tab.I so that the procedure has been supported by quite a comprehensive number of results looking for the minimum NPV among equivalent scenarios. We have selected 54 scenarios for each location, being a few significant cases to show (54=$k * n^m$ where n are the 3 definitions in bold of Tab. I c_p/c_{bat}, c_f and DoA, m are the 3 testing values for each parameter and $k = 2$ the choice on the sizing month PSH1 or PSH2). The comparison shall be performed among similar configurations where upfront costs are the same, while parameters as PSH and SF can range to identify the best solutions, as well as DoA.

Furthermore, there is no need of a too granular choice in parameters because only the most significant, tested by the energy manager, can be used.

Briefly, an overview of the most interesting results of all the run are summarized, for both cases, in Tab. IV, where we can point out that as far as San Diego results concern, the best SF value is 0.1, 0.3 and 0.4 for PSH1, while is 0.1, 0.5 and 0.6 for PSH2, independently on the other parameters (DoA included) but depending on the fuel cost (c_f) and PSH.

In Tab. II the details of the evaluation are reported for Location1: the first outcome relates with the design month: as long as the fuel cost is below \$20/gal, no matter the values of the other parameters, then the best choice is to size the PV field according to the second worst solar month (January); otherwise, it is more convenient to size it against March, which is more similar to the average one in terms of daily irradiance. We can appreciate the difference by looking at the value of NPV^s, slightly lower for the sizing in PSH1 than in PSH2. N_{PV} are similar (≈ 400).

The second observation is focused on the value of the PV curtailed production: while there is a slight improvement in costs if PSH1 is taken as reference, the curtailed PV production is far too large (30 vs. 18.6 MWh/y) and this can be a drawback, unless an alternative use of this extra electricity is available, for instance, for hot water production (so fictitiously increasing P_L of roughly 13.69% on a daily basis).

Results are reported for different SF=0.1, 0.4, 0.6, 1 for PSH1 and PSH2, the inputs are the ones in the simulations reported in Section II and shown in Tab. I with PV panels SunPower SPR-X22-360 rated 360W and the unitary battery being a Relion RB48V200. For the definition of the scenarios in Tab. I, note the data in bold vary over a given range: c_p/c_{bat}, DoA and the fuel cost c_f.

In the cases summarized in Tab. IV, the overarching costs will be different, driven mainly by the battery, but the best solution remains homogeneous, mainly in case of low c_f.

Different conclusions can be drawn for Fairbanks in Tab. III. Here SF, equal to 0.1, is the best solution, even when the fuel cost is \$20/gal and DoA ranges from 1 to 14; nevertheless SF=0.3 turns to be the best sizing solution when sizing according to PSH2 and this solution is also the best among the two sizing strategies. Not only in terms of costs but also in terms of PV curtailment. For Fairbanks the scenario PSH1 is challenging in terms of costs because the PV costs are the overriding item among the three, in scenario PSH2 the costs are more uniform and also more similar in the order of magnitude as San Diego.

According to our KPI (NPV rate), in the far North is more convenient to size PV against higher irradiance months (PSH2), rather than lower.

Among the 54 different Scenarios (c_P rate*DoA*c_f*PSH) considered for San Diego, Tab. IV reports the main outcome, that is $SF = 0.1$ is the best sizing option only when the fuel cost is low (with a range less than \$10/gal), while for higher costs (when c_f 20), the best solution is for $SF = 0.4$ (as the one detailed in Tab. II). Such solutions remain constant when even DoA ranges from 1 to 14 and for San Diego this depends also on the design month (PSH).

For very high c_f, e.g. more than \$100/gal (the results are not reported here, though) then the best solution moves towards higher and higher SF. Very high fuel costs often impact mobile military camps. With the used data for these 54 simulations, other, higher SFs do not seem interesting. And the c_P, always less than 1 does not seem to make any big difference. Accordingly, the battery size matters in terms of total costs (item 2.) but as it does not change with SF, the choice is mainly affected by the other two items (1. and 3.), showing diverging trends.

For Fairbanks the least cost solution is for PSH2 and SF=0.3, nonetheless if PSH1 is chosen to size the PV field than SF=0.1 is the best solution ever (in the investigated ranges).

Here we report only results with c_f up to $20\$/gal$, nonetheless it is desirable to investigate cases where higher fuel costs are considered because they are location-specific and location (see for the far North) is an important variable, as demonstrated by the results presented here.

TABLE II
THE SIMPLIFIED NPV AND NPV-RATE ASSESSMENT (SCENARIO LOCATION1=SAN DIEGO: c_P/c_{bat}=0.7, c_f=20, DOA=4, PSH1=3KWH/(m^2.Y) & PSH2=5KWH/(m^2.Y))

	PSH1=Jan.; SF=0.1	0.4	0.6	1	PSH2=Mar.; SF=0.1	0.4	0.6	1
number of PV panels (N_{PV})	117	**450**	675	1125	72	279	**414**	684
Fuel consumption (AFC, gal/y)	5,488	**1,533**	992	895	6,350	3,413	**1,789**	978
Load fraction from PV=SF*P_L (kWh/d)	60	**240**	360	600	60	240	**360**	600
Pv curtailed (kWh/year)		**30,539**	124,057	349,150			**18,690**	132,306
battery capacity C_r^{CL} (kWh)	3168	**3168**	3168	3,168	3168	3,168	**3,168**	3,168
battery capacity C_r^{L} (kWh)	480	**480**	480	480	480	480	**480**	480
(1.) PV costs ($)	50,544	**194,400**	291,600	486,000	31,104	120,528	**178,848**	295,488
(2.) battery costs-penalty ($)	572,160	**572,160**	572,160	572,160	572,160	572,160	**572,160**	572,160
(3.) annualized OPEX ($ in T_H)	475,232	**132,700**	85,900	77,489	549,859	295,555	**154,933**	84,677
$NPV(F)^s$ = (1.)+(2.)+(3.) ($)	1,097,936	**899,260**	949,660	1,135,649	1,153,123	988,243	**905,941**	952,325
NPV^s over NPV^* (**NPV-rate**)	1.2209	**1.**	1.0560	1.2629	1.2728	1.0908	**1.**	1.0512

TABLE III
THE SIMPLIFIED NPV AND NPV-RATE ASSESSMENT (SCENARIO LOCATION2=FAIRBANKS: c_P/c_{bat}=0.7, c_f=20, DOA=4, PSH1=0.14KWH/(m^2.Y) & PSH2=2KWH/(m^2.Y))

same unit of measurement as Tab. II	PSH1=Jan.; SF=0.1	0.3	0.6	1	PSH2=Sep.; SF=0.1	0.3	0.6	1
number of PV panels	**2,619**	7,857	15,714	26,190	180	**522**	1,035	1,728
Fuel consumption	**2,001**	1,475	958	931	6,079	**3,901**	2,912	2,339
Load fraction on PV=SF*PL	**60**	180	360	600	60	**180**	360	600
PV curtailed	**422,062**	1,613,577	3,420,251	5,843,808	-	**4,795**	93,990	244,295
battery capacity C_r^{CL}	**3,264**	3,264	3,264	3,264	3,168	**3,168**	3,168	3,168
battery capacity C_r^{L}	**480**	480	480	480	480	**480**	480	480
(1.) PV cost	**1,131,408**	3,394,224	6,788,448	11,314,080	77,760	**225,504**	447,120	746,496
(2.) battery costs-penalty	**583,680**	583,680	583,680	583,680	572,160	**572,160**	572,160	572,160
(3.) annualized OPEX	**173,283**	127,724	82,978	80,619	526,410	**337,772**	252,184	202,530
$NPV(F)^s$ =(1.)+(2.)+(3.)	**1,888,371**	4,105,628	7,455,106	11,978,379	1,176,330	**1,135,436**	1,271,464	1,521,186
NPV^s over NPV^* (**NPV-rate**)	**1.**	2.1742	3.9479	6.3432	1.0360	**1.**	1.1198	1.3397

B. Discussion

The proposed methodology offers a valuable decision tool to design isolated microgrids, depending on the location and on several design parameters. It offers a way to navigate the many interwoven design choices which influence the initial cost and future management of the microgrid with the goal to improve resilience on the critical load. This goal is particularly important for critical facilities and these authors have not found in literature any procedure which is as simple and comprehensive as the one proposed here. Although several microgrid sizing methodologies have been proposed in literature, none present a trade-off among the many parameters considered in this paper and their interconnected effects. The Monte Carlo results show that we can get to the best DER sizing solution quicker, once only sensitive parameters -as those identified- are chosen. The results presented in the previous section demonstrate the robustness of the simulated solutions: for instance, we have learned that once PSH has been set, then the best SF depends mainly on the fuel cost, no matter how the values of DoA and c_p/c_{bat} change in the given ranges. The results of the 108 (54 for each location) simulations are all synthesized in Tab. IV and the following evidence is confirmed: there is a trade-off in costs, curtailed energy, PV extension, and battery capacity when sizing a microgrid over different solar months and DoA.

When the PV sizing reference is a month with an average low irradiance (PSH1), if we focus our attention on a given SF, then the number of PV panels and the fuel consumption are respectively higher and lower than the corresponding data, when the sizing month has a higher average irradiance (PSH2). This result can be observed by comparing the first two lines of both Tab. II and III) from left to right.

Although the results for the total cost are less predictable, they indicate a trend when the fuel cost is getting higher and higher, that is, it seems more convenient to size the system on the month, whose irradiation is closer to the annual average. Therefore, the best solution is likely to be found for higher SFs, because those are the solutions when choosing the extreme boundaries of the possible choices. And fuel cost can skyrocket for microgrids in remote locations or harsh climate. For example, the *the fully burdened cost of fuel* can be more than $\$400/gal$ including the total ownership cost of buying, moving and protecting fuel in systems during the most challenging occurrences [23]). Hence, as long as the fuel features a reasonable price (again, the fully burdened cost of fuel) then lower SF are favored and SF=.1 is the least expensive solution. When fuel cost raises or when better solar months are chosen for sizing the PV field, then higher SFs are shown to be less costly. The case of Fairbanks is interesting because the decision parameter NPV-rate, along with NPV^s, can allow to choose the best PSH design, which differs from the one which is best for San Diego. In fact, for San Diego, with more uniform irradiance over the year, the best sizing month is January (according to what [22] suggests), while

for microgrids near the far North ($\approx$ 65 deg), with huge differences in the average monthly irradiance, the best choice lays in the PSH2 part of the table (September), mainly when c_f increases. This is a valuable and not quite expected result.

The matter about how to better assess the resilience is of course open and we are aware that the complexity of the definition does not make a single economic indicator fits for all purposes, but at least it can help once the priorities in the design and long-term management of a microgrid are uniquely established.

TABLE IV
SAN DIEGO & FAIRBANKS: BEST SF FOR THE SELECTED FUEL COST & DESIGN MONTH, $\forall$ DOA & c_P IN THE SET DATA OF TAB.I

	San Diego		Fairbanks	
	PSH1	PSH2	PSH1	PSH2
c_f	SF	SF	SF	SF
4	0.1	0.1	0.1	0.1
10	0.3	0.5	0.1	0.1
20	0.4	0.6	0.1	0.3

IV. Experimental Validation

A stand-alone microgrid was assembled with commercial off-the-shelf (COTS) components including twelve $100W$ $12V$ monoscrystalline PV panels HQST-100D-S [24], a $24V$, $500Ah$ lead-acid deep cycle battery bank SLR500-2 [25], and an Outback FLEXpower control system [26]. The latter is a power electronics system that consists of DC battery monitor, a charge controller, the inverter and charger, a system display and control panel. The charger controller uses a MPPT so the output power of the PV arrays is maximized at all times. The efficiency of the inverter is 90%. The microgrid's main components are shown in Figure 6 and Figure 7. It was designed as a mobile microgrid and it is enclosed inside the container shown in Figure 7, with the PV panels mounted on top and the other components shown in Figure 6 placed inside the container.

Experimental measurements were performed on the COTS microgrid to validate the design method and physics-based model used in Section II and presented in [21]. Over the course of 11 hours, a varying load was applied to the microgrid on a sunny, clear day and the battery bank was discharged from 100% to 30%, its maximum depth of discharge (MDOD). The experimental microgrid DERs were sized and the microgrid's powerflow was simulated using the methodology presented in Section II, then simulations and experimental results were compared and are shown in Figure 8. The PVs are operating quite close to their peak rated voltage of $64V$ from about 10:00 hrs to 17:30 hrs when the insolation is highest and the PV current is above zero. A comparison of the computed and experimental data is shown in Table V. The actual output power produced by the PV panels is lower than expected because there was shading from a building on two of the 12 PV modules during the morning hours of operation.

The battery SOC of both the simulation and the experiment depicted in Figure 8 show an excellent match overall, therefore the experimental measurements validate the calculations of the design tool as well as the physics-based model. Additional experiments and validations can be found in [21].

TABLE V
COMPUTED VS. EXPERIMENTAL DATA

Parameter	**Computed**	**Experimental**
PV Output [Ah/day]	176.7	170.0
PV Output [kWh/day]	4.20	4.16
Battery Output [Ah/day]	318	333
Battery Output [kWh/day]	7.63	7.99

V. Conclusions and Future Work

This paper presents a design methodology and decision support strategy (DSS) to size DERs in stand-alone microgrids with focus on resilience and cost trade-offs. First, design examples are presented for different geographical locations, then the DSS shows how the NPV changes due to the diverging trends on PV and diesel expenditures. Specifically we demonstrate that sizing for different months affects the NPV.

The strength of this procedure lays in an algorithm which is simple to implement and can be easily adapted: for example by including in the NPV other cost variables such as battery degradation, affected by how resilience is formulated.

Another novelty is how we introduced a penalty for downsizing the battery below the target of 14 DoA, by linking it to a simpler rate value (over c_{bat}).

The design methodology was successfully validated by experimental measurements on a COTS microgrid demonstrating that the calculated and simulated battery and PV outputs are in agreement with the experimental measurements.

Acknowledgment

The authors would like to thank Mr. Sonny Rusconi, an Electrical Engineering graduate at the University of Pavia, for his outstanding help with the run of the MonteCarlo simulations.

References

[1] N. Anglani, G. Oriti, and M. Colombini, "Optimized energy management system to reduce fuel consumption in remote military microgrids," *IEEE Transactions on Industry Applications*, vol. 53, no. 6, pp. 5777–5785, 2017.

[2] R. E. Giachetti, C. J. Peterson, D. L. Van Bossuyt, and G. W. Parker, "Systems engineering issues in microgrids for military installations," in *INCOSE International Symposium*, vol. 30, no. 1. Wiley Online Library, 2020, pp. 731–746.

[3] C. D. Rodríguez-Gallegos, O. Gandhi, D. Yang, M. S. Alvarez-Alvarado, W. Zhang, T. Reindl, and S. K. Panda, "A siting and sizing optimization approach for pv–battery–diesel hybrid systems," *IEEE Transactions on Industry Applications*, vol. 54, no. 3, pp. 2637–2645, 2017.

[4] S. Bandyopadhyay, G. C. Mouli, Z. Qin, L. R. Elizondo, and P. Bauer, "Techno-economical model based optimal sizing of pv-battery systems for microgrids," *IEEE Transactions on Sustainable Energy*, 2019.

[5] M. Mehrtash, F. Capitanescu, P. K. Heiselberg, T. Gibon, and A. Bertrand, "An enhanced optimal pv and battery sizing model for zero energy buildings considering environmental impacts," *IEEE Transactions on Industry Applications*, vol. 56, no. 6, pp. 6846–6856, 2020.

[6] X. Wu, W. Zhao, X. Wang, and H. Li, "An milp-based planning model of a photovoltaic/diesel/battery stand-alone microgrid considering the reliability," *IEEE Transactions on Smart Grid*, vol. 12, no. 5, pp. 3809–3818, 2021.

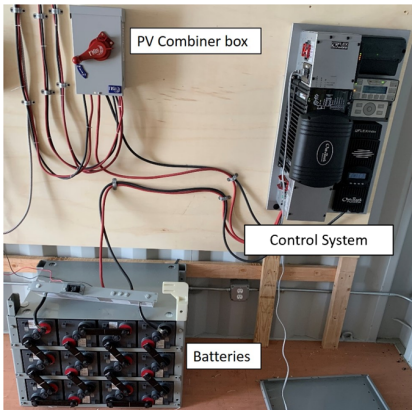

Fig. 6. COTS microgrid set-up

Fig. 7. Microgrid enclosure and PV arrays

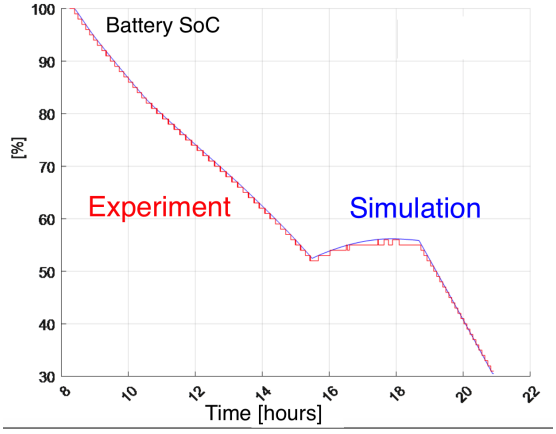

Fig. 8. Simulated vs measured battery SOC

[7] A. A. Z. Diab, H. M. Sultan, I. S. Mohamed, O. N. Kuznetsov, and T. D. Do, "Application of different optimization algorithms for optimal sizing of pv/wind/diesel/battery storage stand-alone hybrid microgrid," *IEEE Access*, vol. 7, pp. 119 223–119 245, 2019.

[8] J. Dong, L. Zhu, Y. Su, Y. Ma, Y. Liu, F. Wang, L. M. Tolbert, J. Glass, and L. Bruce, "Battery and backup generator sizing for a resilient microgrid under stochastic extreme events," *IET Generation, Transmission & Distribution*, vol. 12, no. 20, pp. 4443–4450, 2018.

[9] K. Lai, Y. Wang, D. Shi, M. S. Illindala, Y. Jin, and Z. Wang, "Sizing battery storage for islanded microgrid systems to enhance robustness against attacks on energy sources," *Journal of Modern Power Systems and Clean Energy*, vol. 7, no. 5, pp. 1177–1188, 2019.

[10] B. Zhang, P. Dehghanian, and M. Kezunovic, "Optimal allocation of pv generation and battery storage for enhanced resilience," *IEEE Transactions on Smart Grid*, vol. 10, no. 1, pp. 535–545, 2017.

[11] E. Chatterji and M. D. Bazilian, "Battery storage for resilient homes," *IEEE Access*, vol. 8, pp. 184 497–184 511, 2020.

[12] C. Chen, J. Wang, F. Qiu, and D. Zhao, "Resilient distribution system by microgrids formation after natural disasters," *IEEE Transactions on Smart Grid*, vol. 7, no. 2, pp. 958–966, 2016.

[13] B. Zhang, P. Dehghanian, and M. Kezunovic, "Optimal allocation of pv generation and battery storage for enhanced resilience," *IEEE Transactions on Smart Grid*, vol. 10, no. 1, pp. 535–545, 2019.

[14] A. Hussain, V. Bui, and H. Kim, "A proactive and survivability-constrained operation strategy for enhancing resilience of microgrids using energy storage system," *IEEE Access*, vol. 6, pp. 75 495–75 507, 2018.

[15] J. Marqusee, W. Becker, and S. Ericson, "Resilience and economics of microgrids with pv, battery storage, and networked diesel generators," *Advances in Applied Energy*, vol. 3, p. 100049, 2021. [Online]. Available: https://www.sciencedirect.com/science/article/pii/S266679242100041X

[21] R. Fish, "Design and modeling of hybrid microgrids in arctic environments," Master's thesis, Naval Postgraduate School, 2020, https://calhoun.nps.edu/handle/10945/66072.

[16] N. Anglani, G. Oriti, R. Fish, and D. L. V. Bossuyt, "Design and optimization strategy to size resilient stand-alone hybrid microgrids in various climatic conditions," in *2021 IEEE Energy Conversion Congress and Exposition (ECCE)*, 2021, pp. 210–217.

[17] A. M. Madni, D. Erwin, and M. Sievers, "Constructing models for systems resilience: Challenges, concepts, and formal methods," *Systems*, vol. 8, no. 1, p. 3, 2020.

[18] C. Peterson, D. Van Bossuyt, R. Giachetti, and G. Oriti, "Analyzing mission impact of military installations microgrid for resilience," *Systems*, 2021, in Review.

[19] C. J. Peterson, "Design and modeling of hybrid microgrids in arctic environments," Master's thesis, Naval Postgraduate School, 2019. [Online]. Available: https://calhoun.nps.edu/handle/10945/63493

[20] P. Siritoglou, G. Oriti, and D. L. Van Bossuyt, "Distributed energy-resource design method to improve energy security in critical facilities," *Energies*, vol. 14, no. 10, 2021. [Online]. Available: https://www.mdpi.com/1996-1073/14/10/2773

[22] G. M. Masters, *Renewable and efficient electric power systems*. John Wiley & Sons, 2013.

[23] The Hill. (2009, Oct.) $400 per gallon gas to drive debate over cost of war in afghanistan. [Online]. Available: https://thehill.com/homenews/administration/63407-400gallon-gas-another-cost-of-war-in-afghanistan-

[24] HQST. (2020, July) 100 watt 12 volt monoscrystalline solar panel. [Online]. Available: https://hqsolarpower.com/100-watt-12-volt-monoscrystalline-solar-panel-compact-design-back-order/

[25] GS Battery. (2020, July) Advanced lead deep-cycle batter slr500-2. [Online]. Available: https://d3g1qce46u5dao.cloudfront.net/data_sheet/slr500_brochure.pdf

[26] Outback Power. (2020, July) Outback flexpower one fp1 fxr3048a-01 3,000 watts 48 volts for off-grid and grid-tie. [Online]. Available: https://www.solar-electric.com/outback-flexpower-inverter-system-fp1-fxr3048a-01.html